Structural, bonding, and dynamical properties of liquid Fe-Si alloys: An *ab initio* molecular-dynamics simulation

Tingkun Gu,[1,2] Jingyu Qin,[1] Changye Xu,[3] and Xiufang Bian[1]
[1]*The Key Laboratory of Liquid Structure and Heredity of Materials, Ministry of Education, Shandong University, Southern Campus, Jinan 250061, People's Republic of China*
[2]*School of Electrical and Engineering, Shandong University, Jinan 250061, People's Republic of China*
[3]*School of Physics and Microelectronics, Shandong University, Jinan 250061, People's Republic of China*
(Received 6 December 2003; published 26 October 2004)

Molten Fe-Si alloys have been investigated with an *ab initio* molecular-dynamics technique at 1823 K. Our calculated results are in good agreement with experimental results. Analysis of the static structure shows that the structure of liquid Fe-Si alloys can be divided into four subintervals separated by the compounds $Fe_{0.75}Si_{0.25}$, $Fe_{0.50}Si_{0.50}$, and $Fe_{0.285}Si_{0.715}$. The calculated electronic density of states for liquid Fe-Si alloys indicates that the Fe-Si bonds are due to the hybridization of Fe ($3d$) and Si ($3p$), and there are Si-Si bonds in molten Fe-Si alloys as Si content beyond 70 at. %. The changes of Fe and Si diffusion coefficients with increasing Si content have the same characters as in static structure

DOI: 10.1103/PhysRevB.70.144204 PACS number(s): 61.25.Mv, 71.22.+i, 61.20.Ja

I. INTRODUCTION

The Fe-Si phase equilibrium diagram is complex, including many kinds of intermediate phases, such as Fe_3Si, Fe_2Si, FeSi, $FeSi_2$, and Fe_2Si_5.[1,2] The Fe_3Si compound has DO_3 crystallographic structure and is a kind of magnetic material.[3] ε-FeSi alloy is an excellent magnetic semiconductor with melting point higher than 1683 K.[4,5] β-$FeSi_2$ alloy is known as an excellent thermoelectric material that can be applied in high-temperature air atmosphere.[6] Si is the well-known important semiconductor material.

Fe-Si alloys are one of the fundamental systems in iron and steel making. The thermodynamic activities of Fe and Si show a remarkable negative deviation from Raoult's law,[7] representing a strong interaction between Fe and Si atoms in molten Fe-Si alloys.

To our knowledge there have been several experimental studies of the structure of liquid Fe-Si alloys. Vatolin and Pastuhov[8] suggested that experimental results on molten Fe-Si could be explained by a quasieutectic model based on crystalline FeSi, $FeSi_2$, Fe, and Si. Waseda and Tamaki[9] carried out an x-ray diffraction analysis for molten Fe-Si alloys and obtained three partial structure factors using an anomalous scattering technique. In their results, it was shown that the partial interference functions were nearly independent of the concentration of alloys and that the Fe and Si atoms act, to a first approximation, as hard spheres in molten Fe-Si alloys. Later on, Kita *et al.*[10] carried out an x-ray diffraction study of molten Fe-Si alloys for the whole concentration range at intervals of about 10 at. % Si at temperatures about 50 K above the liquidus. In order to explain the behavior that some structural parameters are invariant with composition, they used the Percus-Yevick equation to obtain the partial structure factors and found good agreement achieved with the partial structure factors derived from experimental data by a concentration method that necessarily involves the assumption that the three partial functions are independent of composition. They believed that the structure of molten Fe-Si alloys in the range up to 40 at. % Si could be, to a first approximation, explained by the random mixture of hard spheres, while for the alloys in the range beyond 50 at. % Si, those features vary with increasing Si concentration. Recently, Sedelmeyer and Steeb[11] presented x-ray diffraction with molten Fe_2Si and $FeSi_2$ alloys of which the pair correlation functions could be modeled using the data of their corresponding crystalline alloys. They suggested that for molten $FeSi_2$ microsegregation into crystallinelike $FeSi_2$ and Si or FeSi and for molten Fe_2Si microsegregation into crystallinelike Fe_2Si and Fe or FeSi exist. Qin[12] carried out an x-ray diffraction analysis for liquid Fe-Si alloys at a constant temperature of 1823 K; details of the experiments will be published elsewhere separately.

Perhaps some one can argue that the conflicting conclusions may come from the lower accuracy in some experiments, which is really true in the early studies, but our experimental results are compatible with that of Kita *et al.* (1982) and Sedelmeyer and Steeb *et al.* (1997). To our knowledge the main reason for the conflicting explanations lies in the complex nature of molten Fe-Si alloys and the lack of reliable partial structural functions. Therefore, the experimental results quoted above are obtained by analyzing the total structural parameters and there are some problems to be solved. (1) There is no unambiguous description for the concentration dependence of the liquid structure of FeSi alloys, especially in the Fe-rich and Si-rich ranges. (2) In all experimental results, the researchers thought that the covalent Si-Si bond would exist in molten Fe-Si alloys as the Si concentration beyond a certain percent. But Kita and Van Zytvel[13] thought this value is 90 at. %, Qin[12] thought this value is 70 at. % and Votalin and Pastuhov[8] thought this value is 50 at. %. (3) The concentration dependence of liquid structure of FeSi alloys confirms the complex character of interatomic interactions in Fe-Si systems, but the experimental results cannot give a sound explanation for this problem since the interatomic interaction in Fe-Si systems is closely related to their electronic structures. To solve these problems,

reliable partial structural functions and electronic structures of liquid FeSi alloys should be given.

To gain reliable partial structural functions and electronic structures of liquid FeSi alloys, we have performed *ab initio* molecular-dynamics (AIMD) simulations. The AIMD simulations are based on density-functional theory[14] (DFT) and the pseudopotential method,[15] following the methods pioneered by Car and Parrinello.[16] DFT is generally accurate for metals and semiconductors, and previous AIMD simulations of liquid metals and alloys have demonstrated close agreement with experimental results.[17–19] It is useful to study the liquid structures of FeSi alloys in different compositions by *ab initio* molecular-dynamics simulations.

The paper is organized as follows: In Sec. II we discuss the theoretical framework, and in Sec. III we present the results of static structure and compare with the experimental and other theoretical results. In Sec. IV we report the electronic structure of liquid Fe-Si alloys. Section V is a discussion of the dynamical properties. The final section is the conclusion.

II. COMPUTATIONAL METHODS

Our calculations have been performed by using the Vienna *ab initio* simulation program VASP.[20,21] The first-principles calculations presented here are based on density-functional theory within the generalized gradient approximation (GGA) of Perdew and Wang,[22] using ultrasoft pseudopotentials of the Vanderbilt type[23,24] to describe the electron-ion interaction. As the electronic ground state is calculated exactly after each ionic move, the system always remains in the adiabatic ground state, which is an evident advantage in MD simulations for metallic system. The simulations are performed in a canonical ensemble by using a Nosé thermostat for temperature control.[25]

Moroni *et al.*[2] have studied the crystalline structure of Fe-Si systems by VASP. They indicate that the GGA improves substantially the agreement with experiment as compared to the local density approximation LDA results. Thus, in all of our calculations we use the GGA functional.

Our simulations for liquid Fe-Si alloys have been performed by using a cubic supercell. For all calculated alloys, the cubic supercell contains 64 atoms. Since many research works imply that a microsegregation phenomenon exists in molten Fe-Si alloys, it is better to study the molten Fe-Si alloys at constant temperature rather than constant overheating temperature. In the constant-temperature scheme, some kinds of aggregation will experience the same temperature in different alloys. Thus, the temperatures are set at constant temperature 1823 K in our simulations and the experimental densities are used.[12] The Γ point alone is used to sample the Brillouin zone of the supercell. The equations of motion are solved via the velocity Verlet algorithm with a time step of 3 fs. The quantities of interest are obtained by averaging over about 3 ps after the initial equilibration taking about 2 ps.

III. STRUCTURAL PROPERTIES

To compare with the experimental results, we have calculated the structure factors of liquid Fe-Si alloys. The partial structure factors $S_{ij}(k)$ are defined by

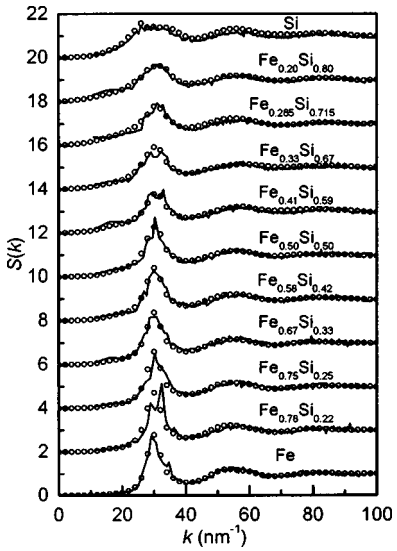

FIG. 1. Calculated total structure factors $S(k)$ of molten Fe-Si alloys (solid lines) compared with the results of experiment (circles, Ref. 12).

$$S_{ij}(k) = \frac{1}{N_i N_j}\left\langle \sum_{\mu=1}^{N_i}\sum_{\gamma=1}^{N_j} e^{ik\cdot(r_\mu - r_\gamma)} \right\rangle. \tag{1}$$

The positions of ions $\{r_\mu\}$ are obtained by our *ab initio* MD simulations; N is the number of ions of the ith species and the brackets $\langle\cdots\rangle$ mean the time average. The total structure factor is then expressed as a linear combination of the partial structure factors $S_{ij}(k)$:

$$S(k) = \sum_i \sum_j c_i^{1/2} c_j^{1/2} \frac{f_i(k) f_j(k)}{c_i f_i^2(k) + c_j f_j^2(k)} S_{ij}(k), \tag{2}$$

where $f_i(k)$ is the atomic scattering factor of the ith species.

The structure factors $S(k)$ thus obtained are compared with the experimental results by x-ray diffraction in Fig. 1. Our results are in good agreement with the experimental results from pure Fe to pure Si.

The structural properties of the liquid system have been inspected by looking at the partial pair correlation functions (PCF's) $g_{\mathrm{FeFe}}(r)$, $g_{\mathrm{FeSi}}(r)$, and $g_{\mathrm{SiSi}}(r)$. The partial PCF's are defined in such a way that, sitting on one atom of the species α, the probability of finding one atom of the species β in the spherical shell $(r \sim r + \mathrm{d}r)$ is $4\pi\rho_\beta g_{\alpha\beta}(r)\mathrm{d}r$, where ρ_β is the number density of the species β.

The partial pair correlation functions are shown in Fig. 2. In any studied composition, the first peak of $g_{\mathrm{FeSi}}(r)$ is higher than the other two, $g_{\mathrm{FeFe}}(r)$ and $g_{\mathrm{SiSi}}(r)$, and its position shifts to smaller r. This indicates that in molten Fe-Si alloys the interaction between Fe-Si is stronger than that between Fe-Fe and Si-Si. Therefore, the liquid Fe-Si alloys are a non-ideal solution and are displayed as a negative deviation from Raoult's law. $g_{\mathrm{FeFe}}(r)$ exhibits dramatic changes with increasing Si concentration, and the magnitude of the main peak decreases and its position shifts to larger r with decreasing Fe concentration, but the second peak shows the opposite feature, its magnitude increases and its position shifts to

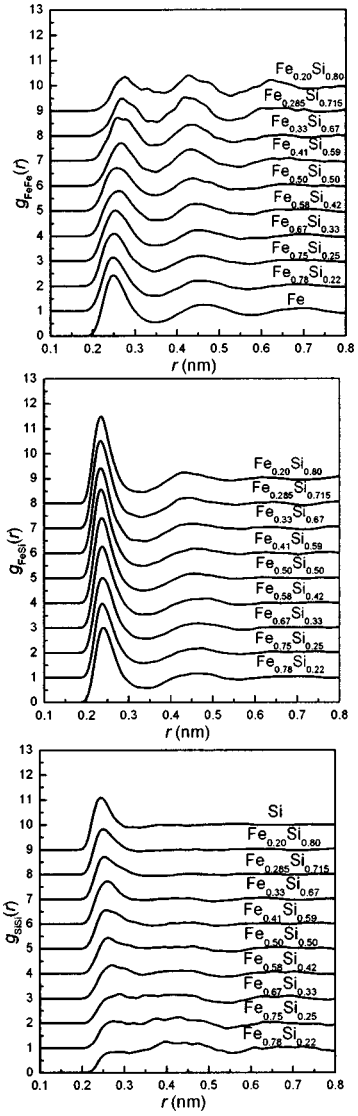

FIG. 2. The partial pair correlation functions of liquid Fe-Si alloys.

smaller r. At Si content beyoned 71.5 at. %, the second peak of $g_{\mathrm{FeFe}}(r)$ is a little higher than the first peak. The $g_{\mathrm{SiSi}}(r)$ has no obvious first peak when the Si content is less than 40 at. %. For alloys with 25 and 22 at. % Si, the second peak in $g_{\mathrm{SiSi}}(r)$ is even a little higher than their first peak. This resembles the Si-Si coordination in DO_3-type Fe_3Si, where no Si atom is the nearest neighbor of a Si atom since they are separated by Fe atoms with a distance as far as 0.399 nm. These features encourage us to think that in molten Fe-Si alloys of both Si-rich and Fe-rich ranges the atoms of the minor specie tend to have more like atoms in the second-coordination shell than in the first-coordination shell.

The total particle-particle correlation is defined by

$$g(r) = \sum_i \sum_j \frac{c_i c_j f_i f_j}{(c_i f_i + c_j f_j)^2} g_{ij}(r), \tag{3}$$

where f_i is the atomic scattering factor. The total pair correlation functions are shown in Fig. 3.

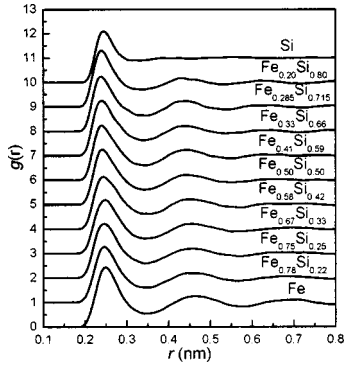

FIG. 3. Total pair correlation functions of liquid Fe-Si alloys.

Given the total and partial pair correlation function, it is possible to estimate coordination numbers as

$$N_{\alpha\beta} = \int_0^{r_{\min}} 4\pi r^2 \rho_\beta g_{\alpha\beta}(r) \mathrm{d}r, \tag{4}$$

where $r_{\min}$ is the first minimum coordinate in $4\pi\rho_\beta g_{\alpha\beta}(r)$ [defined as partial radial distribution function (RDF) in this paper]. The total coordination number can be obtained similarly by Eq. (4). The first peak position r_1 of the RDF—i.e., the nearest-neighbor distance—and the coordination number can be obtained and are given in Figs. 4 and 5. Because the partial radial distribution functions of Si have no obvious first peak in the Fe-rich region, we do not show the nearest-neighbor distance of Si-Si in Fig. 4.

As can be seen from Figs. 4 and 5, the total coordination numbers and nearest-neighbor distances calculated from the total RDF's are in good agreement with experimental results.[10,12] The nearest-neighbor distances r_1 for pure liquid Fe and Si are obtained to be 0.256 nm and 0.250 nm, respectively, which agree well with the results by other investigators.[8,26] It can be seen from Figs. 3 and 4 that when the liquid alloys are in the range up to 40 at. % Si, the total pair correlation functions $g(r)$ have prominent first peaks and successive well-defined maxima, and the nearest-neighbor distances r_1 are nearly invariant with increasing Si content. For liquid alloys with concentrations beyond 50 at. % Si, with increasing Si content, the width of the first peak of $g(r)$ becomes narrower and the nearest-neighbor distance r_1 decreases, which features are consistent with the experimental results obtained by Kita *et al.*[10] For experimental results and

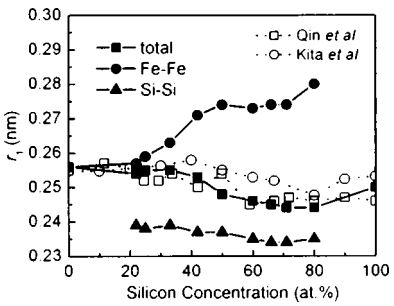

FIG. 4. Composition dependence of the nearest neighbor-distance r_1 for liquid Fe-Si alloys.

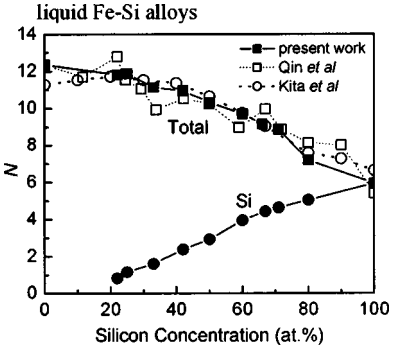

FIG. 5. The total coordination number and the partial coordination number of Si-Si for liquid Fe-Si alloys.

our calculations, the varying trends of total coordination numbers and nearest number distances are consistent. They have a common character that the liquid structure of Fe-Si alloys can be divided into two subintervals with a boundary of $Fe_{0.5}Si_{0.5}$. But in both the Fe-rich and Si-rich ranges, there is a lack of obvious regulations in the total structural parameters. Therefore, using only the total coordination number and nearest number distance as a criterion is not sufficient to describe the liquid structure change with composition for Fe-Si alloys. To investigate the liquid structure of FeSi alloys in detail, the partial structural parameters should be calculated.

The partial nearest-neighbor distances of Fe-Si and Fe-Fe are shown in Fig. 4. The r_1 of Fe-Si in the Fe-rich region is slightly larger than that in the Si-rich region and $Fe_{0.5}Si_{0.5}$ is served as the dividing point. Furthermore, if we draw a straight line from the point (0.0 at. % Si, 0.257 nm) to the point (100.0 at. % Si, 0.246 nm), all the values of r_{FeSi} are obviously below the line. This means that in molten Fe-Si alloys r_{FeSi} cannot be obtained by the binary hard-sphere model, and the shrinking of r_{FeSi} is an indication of the strong interaction between Fe and Si atoms. But the nearest-neighbor distances r_1 of Fe-Fe, having also been shown in Fig. 4, display another characteristic. The behavior that r_{FeFe} increases nonlinearly with Si concentration beyond 25 at. % Si implies that the partial structure functions are not invariant with composition in the range up to 40 at. % Si, as has been suggested by Kita *et al.*[10] The changes of r_{FeFe} with Si concentration can be divided into four subintervals: (1) 0–25 at. % Si, the r_{FeFe} nearly being invariant with composition (0.256–0.259 nm); (2) 25–50 at. % Si, the r_{FeFe} increasing from 0.259 to 0.274 nm; (3) 50–70 at. % Si, the r_{FeFe} nearly being constant in this region; (4) >70 at. % Si, the r_{FeFe} increasing with Si content. The total nearest number distance r_1 is a complex function of the three partial parameters of r_{FeFe}, r_{FeSi}, and r_{SiSi} and composition. From Figs. 2 and 4 we find that though r_{FeFe} increases with Si concentration, r_{FeSi} and r_{SiSi} have the opposite behavior. Then it might be effective to predict the structure of molten Fe-Si alloys by the parameter r_1 when the structure is really like a binary mixture of hard spheres. We also show how the partial coordination numbers of Si-Si change with composition in Fig. 5. They vary nonlinearly as a function of Si concentration; a noteworthy deflection point is observed at 70 at. % Si.

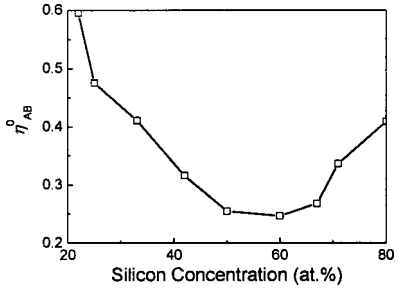

FIG. 6. The short-range order parameters for liquid Fe-Si alloys.

To quantify the ordering, one can use the short-range order parameters as defined by Cargill and Spaepen:[27]

$$\eta_{ij} = \frac{N_{ij}\langle N\rangle}{x_j N_i N_j} - 1, \tag{5}$$

$$\eta^0_{AB} = \eta_{AB}/\eta^{\max}_{AB}, \tag{6}$$

with $\eta^{\max}_{AB} = x_B N_B / x_A N_A$ for $x_B N_B < x_A N_A$ and $\eta^{\max}_{AB} = x_A N_A / x_B N_B$ for $x_A N_A < x_B N_B$, $\langle N\rangle = x_A N_A + x_B N_B$, where x_j is the concentration in j atom and N is the coordination numbers. For complete chemical disorder $\eta^0_{AB}=0$; for complete chemical order $\eta^0_{AB}=1$, for departures from chemical disorder associated with clustering—i.e., chemical preference against AB nearest-neighbor pairs $\eta^0_{AB}<0$.

The chemical short-range order parameters calculated from Eqs. (5) and (6) are shown in Fig. 6. In the whole concentration range the numerical values of η^0_{AB} are always more than zero. It is the signature of existing chemical order between Fe and Si atoms. Likely the numerical values of η^0_{AB} are also separated by the compounds $Fe_{0.75}Si_{0.25}$, $Fe_{0.5}Si_{0.5}$, and $Fe_{0.285}Si_{0.715}$.

From all above calculated results we can arrive at the conclusion that the structure of liquid Fe-Si alloys has experienced 4 times the transformation from pure Fe to pure Si: (1) 0–25 at. % Si, we think in this region Si atoms are distributed randomly in molten Fe-Si alloys and the Fe-Fe bonds are nearly not destroyed by Si atoms; (2) in the range of 25–50 at. % Si, the Fe-Fe bonds have been gradually destroyed by Si atoms and the r_{FeFe} shift to large r, the position of second peak of $g_{\mathrm{FeFe}}(r)$ shift to small r, the total coordination number N, and the short-range order parameter decrease with increasing Si content; (3) 50–70 at. % Si, we consider in this composition range the Fe-Si bonds are most noticeable compared with Fe-Fe and Si-Si bonds, there are nearly no bonds of Fe-Fe and Si-Si; (4) when the Si content is beyond 70 at. %, we think that the covalent Si-Si bonds exist in the liquid alloys. The $g_{\mathrm{SiSi}}(r)$'s have an obvious first peak and the total coordination number N decreases faster than the other three subintervals. The x-ray diffraction experiments of the liquid Fe-Si alloys have been analyzed by Kita and Zytveldl[13] with emphasis on the Si-rich liquid alloys. They presumed a Si-Si covalency both in pure liquid Si and in the Si-rich liquid transition-metal-Si alloys, and for liquid Fe-Si alloys, they thought the covalent Si-Si bonds exist as Si concentration beyond 90 at. %. But Votalin and

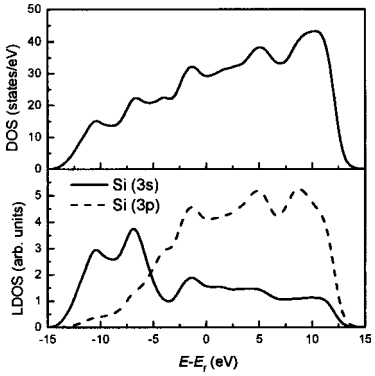

FIG. 7. Total electronic density of states (upper panel) and the local density of states (lower panel) for liquid Si.

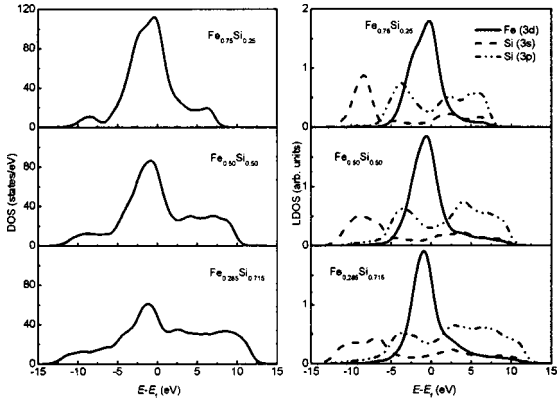

FIG. 8. Total electronic density of states (left panel) and the local density of states for each atomic species (right panel). For clarity, the scale used for the Si LDOS is 4 times that used for the Fe LDOS.

Pastuhov[8] thought this percent is 50 at.%. We will also discuss this problem in the later section by the electronic structure of liquid FeSi alloys.

The physical or thermodynamic properties are closely related with the liquid structure, such as viscosity, electrical resistivity, molar volume, enthalpies, and excess entropies of mixing. The large negative enthalpies and excess entropies of mixing are found in molten Fe-Si alloys.[28] This indicates that there is intensive interaction between Fe and Si atoms. Analyzing the concentration dependence of the partial and integral enthalpies and excess entropies of mixing in molten Fe-Si alloys, we find that the minimum of integral enthalpies (excess entropies) is at about 50 at. % Si and the evident deflection points of partial enthalpies (excess entropies) are found at about 25 and 70 at. % Si. Thus, our deduction on the structure of liquid Fe-Si system derived from *ab initio* molecular-dynamics simulations corresponds well with suggestions given by the variation of these properties with composition.

IV. ELECTRONIC STRUCTURE

The structure behavior of the system can be understood in terms of the electronic structure. Here we have investigated the electronic density of states (DOS). Having in mind a tight-binding interpretation of the chemical bonds among the atoms, it is useful to inspect the local density of states (LDOS)—i.e., the DOS for each atomic species decomposed into angular-momentum-resolved contributions. The (l,m) angular momentum component of the atom i is the projection onto the spherical harmonic (l,m) of all the wave functions in a sphere of radius R centered on the atom i (Ref. 29).

Upon melting the structure of Si goes from an open structure with coordination number equal to 4 to a more compact liquid and the coordination number exceeding 6 (Ref. 9, undergoing a semiconductor-to-metal transition. In Fig. 7, the DOS of liquid Si displays metallic behavior as evidenced by the absence of a gap at the Fermi level E_f and our result is consistent with other *ab initio* calculations.[17] If making a further investigation of the LDOS of liquid Si, we find there is a nice splitting of the 3*s* level, a broadening of 3*p* level, and overlaps between 3*s* and 3*p* bands. It is evident that there is a persistence of covalent bonding in liquid Si.

The calculated electronic DOS and LDOS for three compositions $Fe_{0.75}Si_{0.25}$, $Fe_{0.50}Si_{0.50}$, and $Fe_{0.285}Si_{0.715}$ are displayed in Fig. 8, referring all the energies to the Fermi energy. The Fe (4*s*), Fe (4*p*), and Si (3*d*) orbits are not shown because they contribute small to the DOS. There is a small peak at −8 eV, which comes from the Si (3*s*) orbital and becomes more broadening with increasing Si content up to 50 at. % and splits into two peaks at 71.5 at. %. The main broad peak extending from ≈ -5 eV to $\approx +5$ eV results from Si (3*p*) and Fe (3*d*) orbits, and this means the hybridization of Si 3*p* with Fe (3*d*) states exists in liquid Fe-Si alloys. The Si (3*p*) band has two peaks. One at about −5 eV is the bonding state and the other at +5 eV is the antibonding state with Fe (3*d*). The splitting of the Fe-Si bonding and antibonding levels is a measure of the strength of the bonds. Since it is larger than the broadening of the Fe (3*d*) band, we argue that the Fe-Si bond is stronger than the Fe-Fe one. This is consistent with the results of the PCF's described in the previous section in the sense that the Fe-Si distance is lower than the Fe-Fe one.

To explain the features of DOS and LDOS in liquid FeSi alloys, we have calculated the LDOS of Si in different environment. The first Si atom named Si_1 has been chosen so that there are no other Si atoms and only four Fe atoms within at the distance less than 0.25 nm, while the second Si atom named Si_2 has been chosen so that there are two Si and two Fe atoms in the nearest-neighbor shell. In this way Si_1 makes no bonds with other Si atoms and only bonds with Fe atoms, while Si_2 makes bonds with other Si atoms. Figure 9 displays the calculated LDOS for Si_1 and Si_2 atoms. For the Si_1 atom (no silicon bonds) a sharpening of both the 3*s* and 3*p* peaks and almost no overlaps between them can be observed. In this case the Si_2 is close to other two Si atoms, and there are more overlaps between 3*s* and 3*p* orbits and a nice splitting of 3*s* level and a splitting or broadening of the 3*p* level. Thus, a splitting of Si (3*s*), a splitting or broadening of the Si (3*p*), and overlaps between Si (3*s*) and Si (3*p*) result from covalent Si-Si bonds.

In order to investigate the variation of Fe-Fe bonds in liquid FeSi alloys, we display the Fe (3*d*) band for two se-

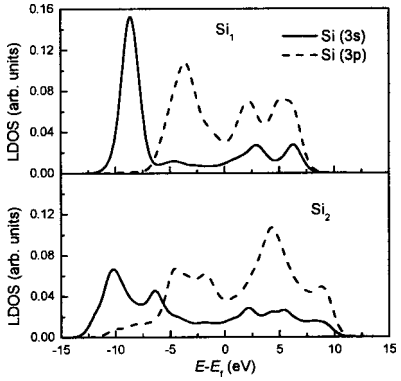

FIG. 9. LDOS for two selected Si atoms.

lected Fe atoms in Fig. 10. Fe_1 has three Fe and one Si atoms within a distance of 0.25 nm and Fe_2 has only four Si atoms within the same distance. A comparison of the two bands clearly shows that the Fe_1 has a broader peak in 3*d* band with respect to Fe_2, but the Fe_2 (only surrounded by Si atoms) has a more extensive tail resulted from the *pd* hybridization as in crystal state.[30]

In conclusion, we find that the overall features of Si 3*s* and 3*p* of $Fe_{0.75}Si_{0.25}$ are the same as those of Si_1 and the peak of Fe 3*d* band is more broadening than that of $Fe_{0.50}Si_{0.50}$ and $Fe_{0.285}Si_{0.715}$. Thus, we can say that there are no Si-Si bonds as the Si content less than 25 at. % and only Fe-Fe and Fe-Si bonds exist in the liquid state. This conclusion is consistent with the result of no obvious first peak in $g_{SiSi}(r)$ as the Si content less than 25 at. %. For $Fe_{0.50}Si_{0.50}$, the peak of the Fe 3*d* band becomes narrower and its tail becomes more extensive, and Si 3*s* and 3*p* bands become more broadening than those of $Fe_{0.75}Si_{0.25}$. Thus, the concentration of Fe-Fe bonds decreases obviously from 25 to 50 at. % Si. As the Si content up to 70 at. %, a splitting of Si 3*s* and a broadening of Si 3*p* as well as more overlaps between them are found, and the Fe 3*d* band becomes narrower and more symmetrical than that of $Fe_{0.75}Si_{0.25}$ and $Fe_{0.50}Si_{0.50}$. When comparing the bands of Si 3*s* and 3*p* of $Fe_{0.285}Si_{0.715}$ with that of Si_2, we find that there are similar features between them. Thus, there are covalent Si-Si bonds in liquid Fe-Si alloys as Si content more than 70 at. %.

V. DYNAMICAL PROPERTIES

We studied the diffusion of atoms in the liquid by calculating the time-dependent mean-square displacement (MSD) defined in the usual way for species α as

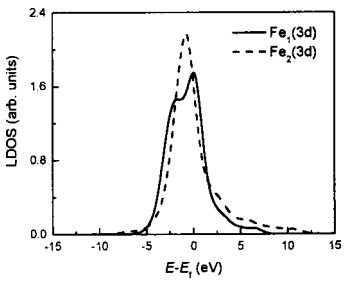

FIG. 10. LDOS for two selected Fe.

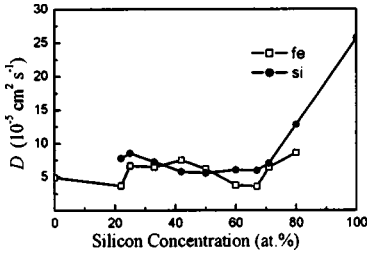

FIG. 11. The diffusion coefficients of Fe and Si for liquid Fe-Si alloys.

$$\langle \Delta r_\alpha(t)^2 \rangle = \frac{1}{N_\alpha} \left\langle \sum_{i=1}^{N_\alpha} |\mathbf{r}_{\alpha i}(t+t_0) - \mathbf{r}_{\alpha i}(t_0)|^2 \right\rangle, \tag{7}$$

where the sum goes over all N_α atoms of species α, t_0 is an arbitrary time origin, and the angular brackets denote a thermal average or equivalently an average over time origins. For diffusing liquids the MSD is linear in t for large time, and the slope is proportional to the diffusion coefficient D_α of species α:

$$\langle \Delta r_\alpha(t)^2 \rangle \rightarrow 6D_\alpha t + B_\alpha, \tag{8}$$

where B_α is constant.

We calculated the MSD of Fe and Si atoms for 11 compositions by averaging over the atoms of each species and over time origins. The estimated diffusion coefficients are reported in Fig. 11. The D_{Fe} of pure liquid Fe is 4.9×10^{-5} cm^2 s^{-1} at temperature 1823 K and $\rho = 7.02$ g cm^{-3}, which is in agreement with the other theoretical result $D_{Fe} = 6.9 \times 10^{-5}$ cm^2 s^{-1} at 1800 K and $\rho = 6.838$ g cm^{-3}.[31] The D_{Si} of pure liquid Si is 2.5×10^{-4} cm^2 s^{-1}, in good agreement with other *ab initio* calculations using different thermostats or initial conditions.[32,33] Comparing D_{Fe} with D_{Si}, we find in the range 0–30 at. % Si, $D_{Fe} < D_{Si}$; 30–50 at. % Si, $D_{Fe} > D_{Si}$; 50–70 at. % Si, $D_{Fe} < D_{Si}$; when the Si content beyond 70 at. %, D_{Si} increases rapidly. The dynamics properties are consistent with the results obtained from static structure analysis.

VI. CONCLUSION

We have used *ab initio* molecular-dynamics simulations based on density-functional theory within the GGA for the exchange correlation energy and ultrasoft pseudopotentials to simulate liquid FeSi alloys at 1823 K. Our calculated structure factors are in good agreement with the experimental data in any composition. From calculation results, we extract reliable structural parameters including total and partial pair correlation functions, nearest-neighbor distances, and coordination numbers. To investigate the electronic structure, we have also calculated the density of states and local density of states for liquid FeSi alloys. The diffusion coefficients of Fe and Si atoms in liquid FeSi alloys are also obtained from calculated results. Analyzing these results, we can get conclusions as follows.

(1) Different from the conclusion of Kita *et al.* obtained from x-ray diffraction, our calculated structural parameters

indicate that the liquid structures of FeSi alloys vary with increasing Si as Si content less than 40 at. %. The analysis of the structural parameters shows that the structure of molten Fe-Si alloys can be divided into four subintervals separated by the compounds $Fe_{0.75}Si_{0.25}$, $Fe_{0.50}Si_{0.50}$, and $Fe_{0.285}Si_{0.715}$. Our deduction of the structure of liquid FeSi alloys derived from *ab initio* molecular-dynamics simulations corresponds well with the composition dependence of the enthalpies and excess entropies of mixing. The calculated diffusion coefficients of Fe and Si atoms also indicate that our suggestion for liquid FeSi alloys is reasonable.

(2) From these behaviors of $g_{SiSi}(r)$ and the composition dependence of the partial coordination number of Si-Si, we deduced that the covalent Si-Si bonds exist in liquid FeSi alloys as Si content beyond 70 at. %. This suggestion is also confirmed by the character of local electronic density of states of liquid $Fe_{0.285}Si_{0.715}$, that a splitting of the Si 3*s* level and a broadening of the 3*p* level as well as more overlaps between them are found.

(3) The calculated electronic structures of molten FeSi alloys indicate that the interaction of Fe-Si atoms are originated from the hybridization of Fe 3*d* and Si 3*p* bands. The Si atoms form bonding and antibonding states with neighboring Fe atoms and the Fe-Si bond is stronger than the bond between Fe atoms. As Si content increasing, the varieties in Fe 3*d*, Si 3*s*, and 3*p* orbitals are consistent with those characters found in structure.

ACKNOWLEDGMENTS

This work was supported by the National Natural Science Foundation of China (Grant No. 50231040) and the Natural Science Foundation of Shandong Province (Project No. Z2001F02)

[1] O. Kubaschewski, *Binary Alloy Phase Diagrams*, edited by T. B. Massalski (ASM, Metal Park, Ohio, 1986), p. 1108.
[2] E. G. Moroni, W. Wolf, J. Hafner, and R. Podloucky, Phys. Rev. B **59**, 12 860 (1999).
[3] J. Kudrnovský, N. E. Christensen, and O. K. Andersen, Phys. Rev. B **43**, 5924 (1991).
[4] S. Paschen, E. Felder, M. A. Chernikov, L. Degiorgi, H. Schwer, H. R. Ott, D. P. Young, J. L. Sarrao, and Z. Fisk, Phys. Rev. B **56**, 12 916 (1997).
[5] T. Jarlborg, Phys. Rev. B **51**, 11 106 (1995).
[6] I. Nishida, Phys. Rev. B **7**, 2710 (1973).
[7] N. S. Gingrich, Rev. Mod. Phys. **15**, 90 (1943).
[8] N. A. Vatolin and E. A. Pastuhov (unpublished).
[9] Y. Waseda and S. Tamaki, Commun. Phys. (London) **1**, 3 (1976).
[10] Y. Kita, M. Zeze, and Z. Morita, Trans. ISIJ **22**, 571 (1982).
[11] B. Sedelmeyer and S. Steeb, Z. Naturforsch., A: Phys. Sci. **52**, 415 (1997).
[12] Qin Jingyu, Acta Metallurgica Sinica (to be published).
[13] Y. Kita and J. B. Van Zytveldl, J. Phys.: Condens. Matter **6**, 811 (1994).
[14] R. O. Jones and O. Gunnarsson, Rev. Mod. Phys. **61**, 689 (1989).
[15] J. C. Phllips, Phys. Rev. **112**, 685 (1958); M. T. Yin and M. L. Cohen, Phys. Rev. B **25**, 7403 (1982).
[16] R. Car and M. Parrinello, Phys. Rev. Lett. **55**, 2471 (1985).
[17] I. Štich, R. Car, and M. Parrinello, Phys. Rev. Lett. **63**, 2240 (1989).
[18] G. Kresse and J. Hafner, Phys. Rev. B **48**, 13 115 (1993).
[19] G. Kresse, J. Non-Cryst. Solids **312–314**, 52 (2002).
[20] G. Kresse and J. Furthmüller, Comput. Mater. Sci. **6**, 15 (1996).
[21] G. Kresse and J. Furthmüller, Phys. Rev. B **54**, 11 169 (1996).
[22] Y. Wang and J. P. Perdew, Phys. Rev. B **44**, 13 298 (1991).
[23] D. Vanderbilt, Phys. Rev. B **41**, 7892 (1990).
[24] G. Kresse and J. Hafner, J. Phys.: Condens. Matter **6**, 8245 (1994).
[25] S. Nose, J. Chem. Phys. **81**, 511 (1984).
[26] Y. Waseda, *The Structure of Non-crystalline Materials: Liquids and Amorphous Solids* (McGraw-Hill, New York, 1980).
[27] G. S. Cargill and F. Spaepen, J. Non-Cryst. Solids **43**, 91 (1981).
[28] V. T. Witusiewicz, J. Alloys Compd. **221**, 74 (1995).
[29] A. Eichler, J. Furthmüller, and G. Kresse, Surf. Sci. **346**, 300 (1996).
[30] K. A. Mäder, H. von Känel, and A. Baldereschi, Phys. Rev. B **48**, 4364 (1993).
[31] P. Protopapas, H. C. Andersen, and N. A. D. Parlee, J. Chem. Phys. **59**, 15 (1973).
[32] I. Štich, R. Car, and M. Parrinello, Phys. Rev. B **44**, 4262 (1991).
[33] V. Godlevsky, J. R. Chelikowsky, and N. Troullier, Phys. Rev. B **52**, 13 281 (1995).